Sloshing of Cylindrical Tank due to Seismic Acceleration

Yasumasa Shoji and Hidenori Munakata

Chiyoda Advanced Solutions Corporation

Technowave 100 Bldg. 1-25, Shin-Urashima-cho, 1-chome,

Kanagawa-ku, Yokohama 221-0031, Japan

Abstract: *Cylindrical tanks are subjected to the seismic loads in certain countries, for example in Japan. The sloshing of these tanks is very important to consider the integrity of the containers. This phenomenon, however, is an interaction of structure and the fluid, namely oil, and is difficult to be analyzed using computer simulation codes. Owing to the FSI capability of Abaqus and Fluent via MpCCI, the phenomenon has been within the range of simulation. Authors tried to analyze the sloshing using the real seismic acceleration at Hachinohe earthquake in Japan and report the result.*

Keywords: *Fluid-Structural Interaction, FSI, Sloshing, cylindrical tank, earthquake, MpCCI*

1. Introduction

In Japan there are a lot of earthquakes in a year, and may be a disaster with remarkable damages in every 2 or 3 years. Accordingly, any plants of refinery, petrochemical, chemical and so on in Japan are designed and constructed to endure these seismic loads. In these plants, as the equipment called "pressure vessels" are usually operated under high pressure and high temperature, their designs are determined to have sufficient integrity for these operating loads rather than for the seismic loads, except in their supporting parts. On the other hand, cylindrical tanks containing oil, especially crude oil, are usually operated under atmospheric pressure and temperature, and the integrity is determined by the seismic loads. This design allows thin wall thickness, and the interaction with the contained fluid may be more easily to occur. In the event of earthquake, the interior liquid may slosh resulting in the damage of the wall or roof of the cylindrical tank, or resulting in the spilling of the fluid which may cause a disastrous fire.

As noted above the interaction between the cylindrical tank and the liquid is more likely to occur and the design codes (KHK, 2006) require the consideration of liquid sloshing based on the historical researches and experiences (Housner, 1954, Jacobsen, 1949 and YNU, 2007). The researches were based on experiment, tests and the theoretical works using potential theories of the fluid, and the fluid-structural interaction (FSI) has not been sufficiently considered. Especially in the theoretical works, in nature, the condition where the wave is too high to be handled in the potential theories was not considered. Recently some researches are taken FSI into account, but no paper is yet to be published using Abaqus code.

In this paper, the FSI capability of Abaqus coupling between Fluent code via MpCCI (ABAQUS, 2006, FLUENT 2005 and SCAI, 2006) is used and analyzed the sloshing of the cylindrical tanks. They are subjected to the real seismic load (acceleration) recorded at the Hachinohe earthquake.

2. Analysis Objects

Two types of tanks were analyzed. The tanks are “virtual” tanks, and one is 6m in diameter and the other one is 50m in diameter.

2.1 Smaller tank

This is a closed tank with a fixed roof. It is 6m in diameter and 3m in height. The depth of the water is 2m. The wall thickness is 20mm. The Hachinohe earthquake wave was used as the seismic load. For this tank, two types of acceleration were used. In the first case, the acceleration was applied to the water, and in the second case the seismic load was applied to the tank base. For both the cases, the interaction between liquid and the structure was considered.

2.2 Larger Tank

This is an open tank without a roof. The dimensions are 50m in diameter and 20m in height, and the oil depth is 15m. The wall thickness is assumed as 25mm for simplicity, although the real wall thickness varies along the elevation. Although the liquid is normally covered by any type of roof, typically a floating roof for this type of larger tanks, to prevent liquid spilling, the roof is neglected in this analysis and the liquid has free surface. In this situation, the sloshing of the liquid and the deformation of the structure were analyzed.

The seismic load is Hachinohe earthquake as applied for the smaller tank. As a trial, this load is doubled in one case to examine the nonlinearity of the sloshing, and in another case the rigid wall tank was also analyzed to investigate the effectiveness of the FSI.

3. Analysis Method and Analytical Model

In any cases, the Abaqus inputs are constructed as follows:

(1) Step 1: The static Abaqus-only step. The hydrostatic pressure of the liquid is applied to the Abaqus model and the tank is deformed initially without any interaction with CFD code.

(2) Step 2: The dynamic FSI step. This is a coupled step with Fluent using MpCCI. The deformation of the step 1 is transferred to Fluent, and Fluent calculates the static pressure of oil based on the deformed tank shape. The hydrostatic pressure is replaced by the fluid pressure from the initial (static) analysis of Fluent in the first increment of the Abaqus analysis. This consideration allows the continuity of the deformation-pressure status in the initial condition of this dynamic step.

The recorded Hachinohe earthquake is shown in Figure 1.

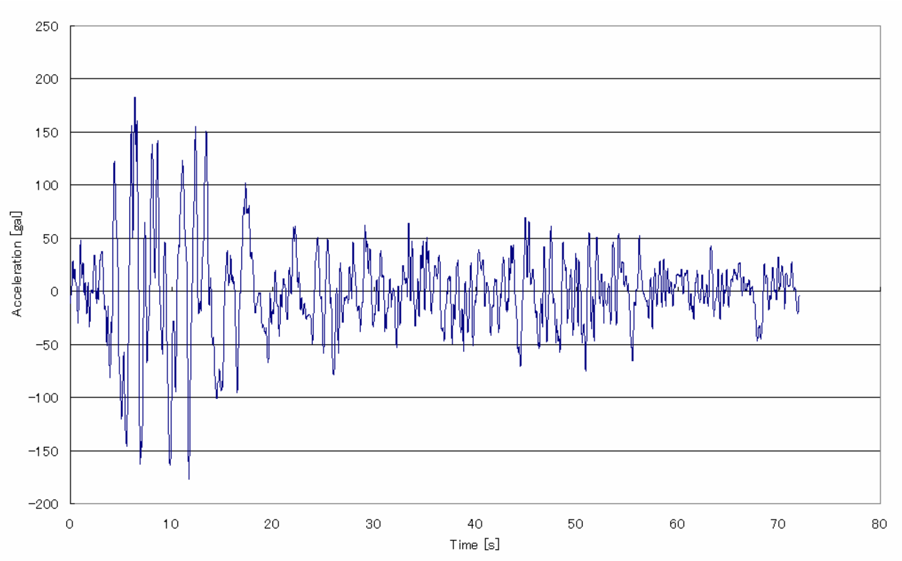

Figure 1. Hachinohe earthquake recorded acceleration.

3.1 Smaller Tank

For this model, the wall was modeled by the solid elements (C3D8I). The analytical model is shown in Fig. 2. The fluid is assumed as water and air.

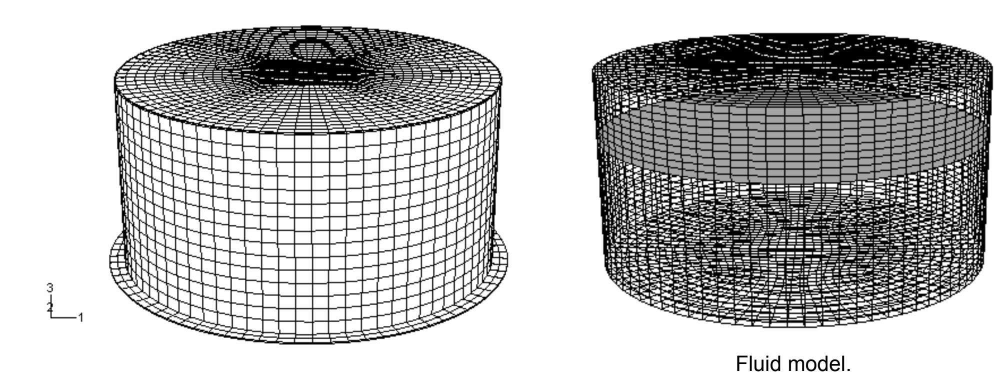

Structural model. Fluid model.

Figure 2. Analytical model of the smaller tank.

The material properties are shown in Table 1.

Table 1 Material Properties for Smaller Tank

Young's modulus	2E11 Pa
Poisson's ratio	0.3
Density of Wall	7800kg/mm3
Density of Water	998.2kg/mm3
Density of Air	1.225 kg/mm3
Viscosity of Water	1.003E-3kg/m s
Viscosity of Air	1.7894E-5kg/m s

The versions of the codes are: Abaqus 6.5-4, Fluent 6.2.16 and MpCCI 3.0.4

3.2 Larger Tank

In this model the tank wall was modeled with shell elements (S4R). The analytical model is shown in Fig. 3. This model is more realistic and the liquid represents oil.

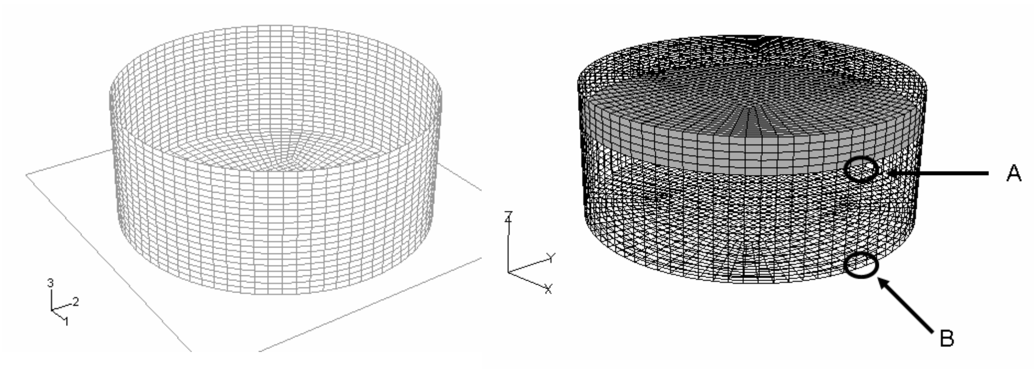

Structural model. Fluid model.

Figure 3. Analytical model of the larger tank.

The material properties are as shown in the Table 2.

Table 2 Material Properties for Larger Tank

Young's modulus	2E11 Pa
Poisson's ratio	0.3
Density of Wall	7800 kg/mm3
Density of Oil	850 kg/mm3
Density of Air	1.225 kg/mm3
Viscosity of Oil	0.048 kg/m s
Viscosity of Air	1.7894E-5 kg/m s

Basically the surface of the liquid is modeled as free surface. A rigid wall case was also analyzed for the reference. The previous researches using potential theory assume that the tank is rigid, and other previous works using CFD codes also employed rigid wall to obtain the behavior of the liquid when it is subjected to the earthquake. The reference rigid-wall analysis case corresponds to these works. The effectiveness of FSI can be examined when we compare the rigid wall results and the flexible wall results.

The version were: Abaqus 6.6-6, Fluent 6.2.16 and MpCCI 3.0.5

4. Analysis Results

4.1 Smaller Tank

Two different loading cases were analyzed. In one case, the seismic load was applied to the fluid and in the other case, the load was applied to the tank base. The analytical results were almost the same. Only the beginning of the response is slightly different, and this is considered to be caused by the effect of the flexibility of the tank. As the stiffness of this tank is rather large, two cases are almost identical in the whole stage. The results are shown in Figures 4 and 5. Figure 4 denotes the liquid surface and the tank deformation at 6.66, 10.98 and 12.16 seconds after the hit of the earthquake. Figure 5 is the Von-Mises stress at the same timing. In this small tank, the wave height is relatively large, and reached to the ceiling. The stress of the liquid-accelerated case is smaller than the base-accelerated case, as the inertia of the tank is not considered, although the wave pressure is almost identical.

4.2 Larger Tank

The analytical results with free surface are shown in Figs. 6 and 7. Figure 6 is the shape of the liquid surface and the deformation of the tank, and Fig. 7 indicates the results of Von-Mises stress. "(a)" indicates the case of original Hachinohe earthquake and "(b)" is the case of doubled acceleration load. These plots are at 6.28, 9.70 and 12.58 seconds after the earthquake reached to the tank. When the acceleration becomes larger, the wave shape differs from what is estimated in the potential theory, as nonlinearity becomes non-negligible. This insists that the potential theory for sloshing has a limit to adapt, and FSI type of analysis is required to estimate a large sloshing behavior for a high wave a priori. Figure 7 shows the vertical displacement of the edge of the liquid free surface (point A of Figure 3). It includes the wave height of the rigid tank, the deformable tank with the original seismic acceleration, the deformable tank with doubled acceleration and the potential theory. The result of the doubled load case is divided by 2 for the normalization purpose. The method to obtain the wave height and the pressure will be addressed in

Section 5, Discussion. This figure shows the difference of the results between the analysis methods.

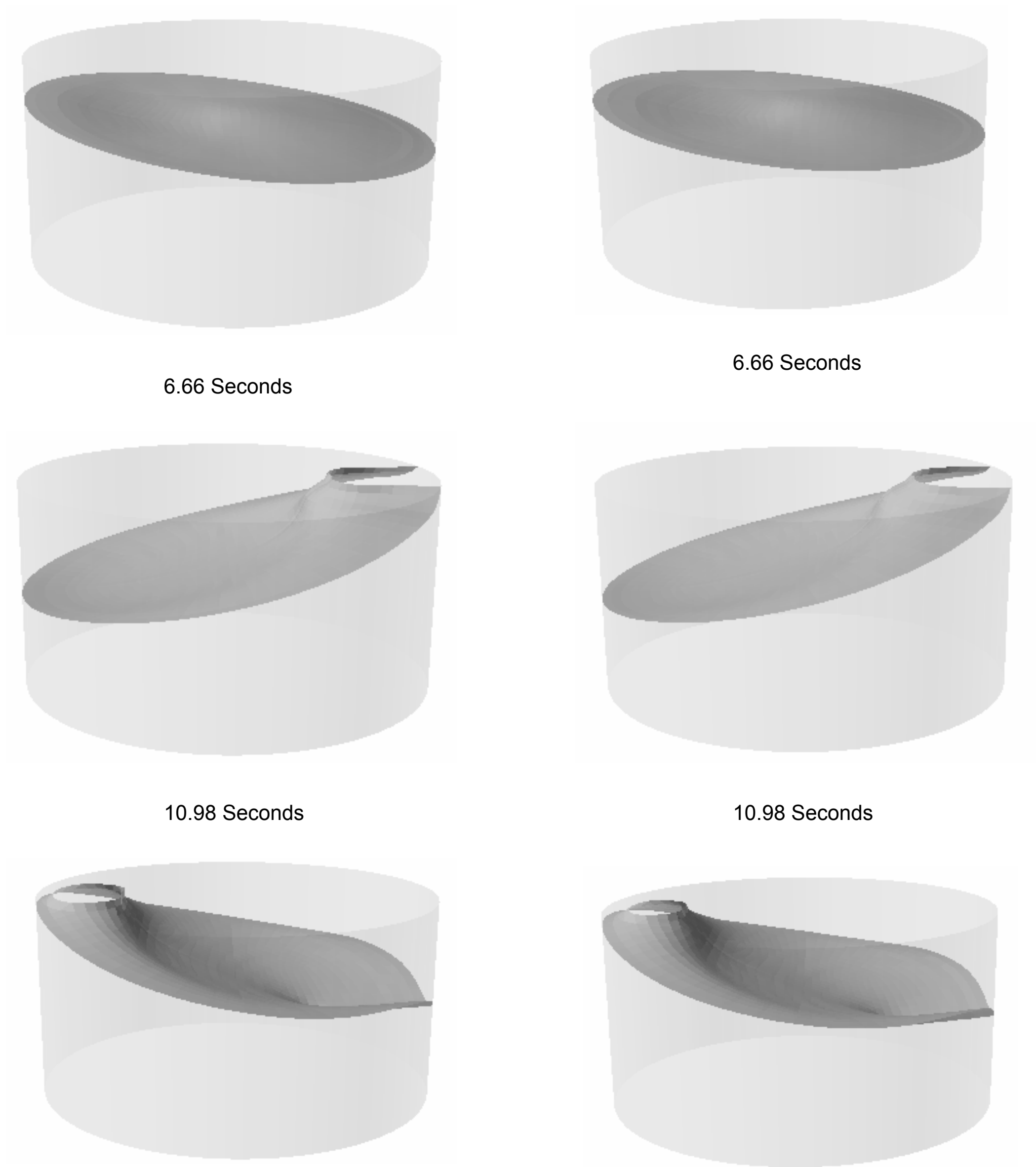

6.66 Seconds 6.66 Seconds

10.98 Seconds 10.98 Seconds

12.16 Seconds 12.16 Seconds

(a) Liquid accelerated (b) Base accelerated

Figure 4. Liquid Surface of smaller tank.

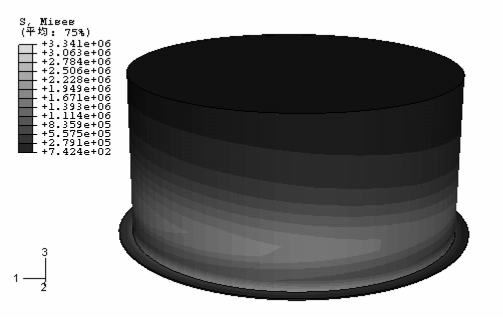

6.66 Seconds

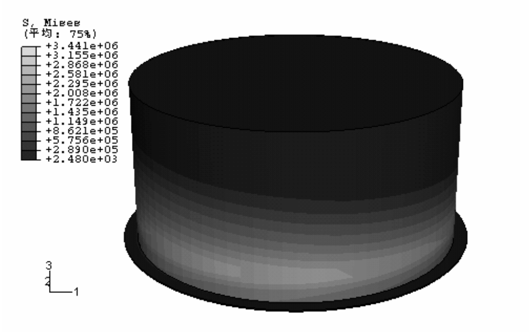

6.66 Seconds

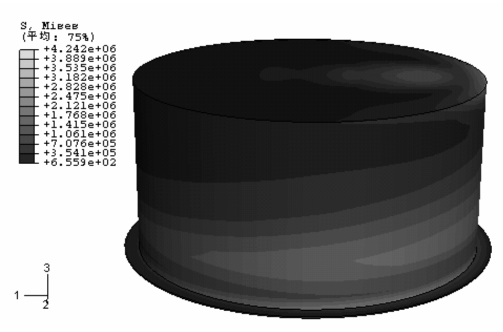

10.98 Seconds

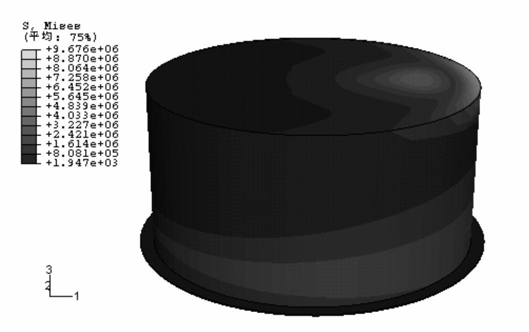

10.98 Seconds

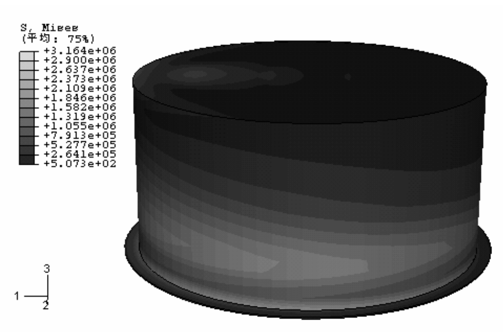

12.16 Seconds

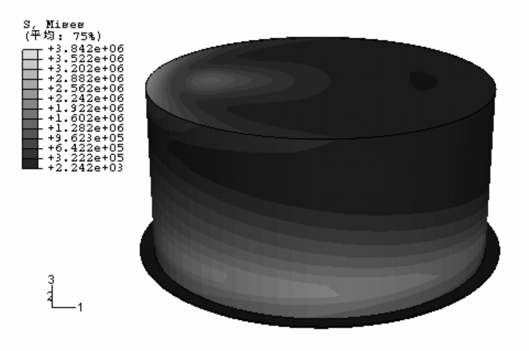

12.16 Seconds

(a) Liquid accelerated

(b) Base accelerated

Figure 5. Mises stress of smaller tank.

A slight difference between the original and the doubled loads shows the existence of the nonlinearity of sloshing. Figure 9 is the pressure of the tank bottom (point B of Figure 3) of the 4 cases as shown in Figure 8. The difference is also seen.

5. Discussion: Comparison with the potential theory

The wave height of the free surfaces (shown in Figure 8) and the pressure at the bottom (shown in Figure 9) were obtained. The wave height and the pressure are derived from the Equation 1 and 2, respectively when potential theory is employed.

$$\Delta P(r,\theta,z,t) = -\rho\left[\sum_i \beta_i J_1\left(\frac{\varepsilon_i r}{R}\right)\cosh\left(\frac{\varepsilon_i z}{R}\right)\ddot{\mathrm{q}}_{\mathrm{i}}\,\mathrm{R} + \mathrm{r}\,\ddot{\mathrm{x}}\right]\cos\theta, \quad (1)$$

$$\eta(r,\theta,t) = -\frac{1}{g}\left[\sum_i \beta_i J_1\left(\frac{\varepsilon_i r}{R}\right)\cosh\left(\frac{\varepsilon_i H}{R}\right)\ddot{\mathrm{q}}_{\mathrm{i}}\,\mathrm{R} + \mathrm{r}\,\ddot{\mathrm{x}}\right]\cos\theta, \quad (2)$$

where,

$$\beta_i = \frac{2}{(\varepsilon_i^2 - 1)J_1(\varepsilon_i)\cosh\left(\frac{\varepsilon_i H}{R}\right)},$$

$$\ddot{\mathrm{q}}_{\mathrm{i}}(t) = \frac{\omega_i^2(1-2\varsigma^2)}{\omega_d}\int_0^t \ddot{\mathrm{x}}(\tau)e^{-\varsigma\omega_i(t-\tau)}\sin\omega_{\mathrm{d}}(\mathrm{t}-\tau)\mathrm{d}\tau$$

$$+2\varsigma\omega_0\int_0^t \ddot{\mathrm{x}}(\tau)e^{-\varsigma\omega_i(t-\tau)}\cos\omega_{\mathrm{d}}(\mathrm{t}-\tau)\mathrm{d}\tau,$$

$$\omega_d = \omega_i\sqrt{1-\zeta^2}$$

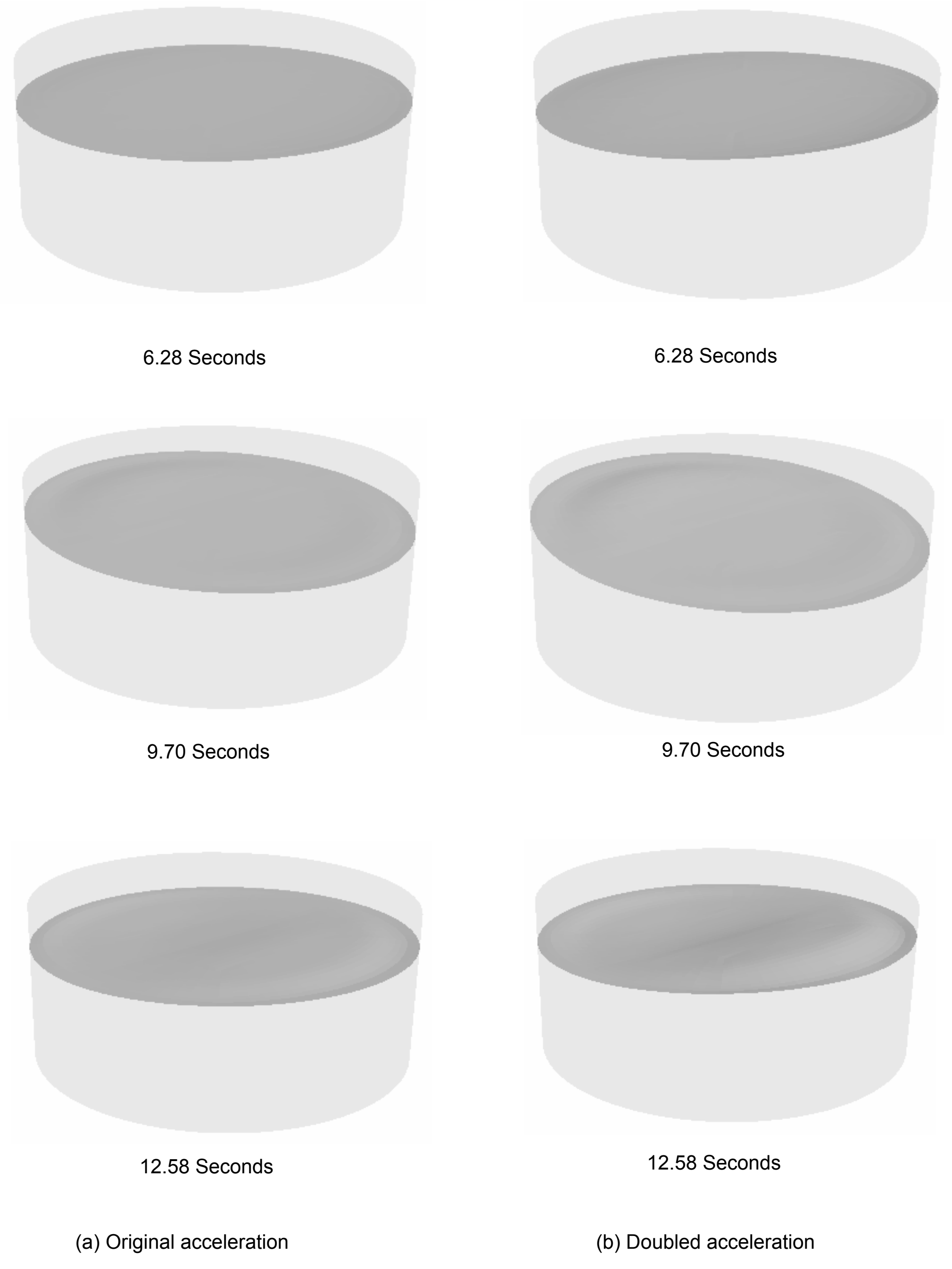

(a) Original acceleration (b) Doubled acceleration

Figure 6. Liquid Surface of deformable larger tank.

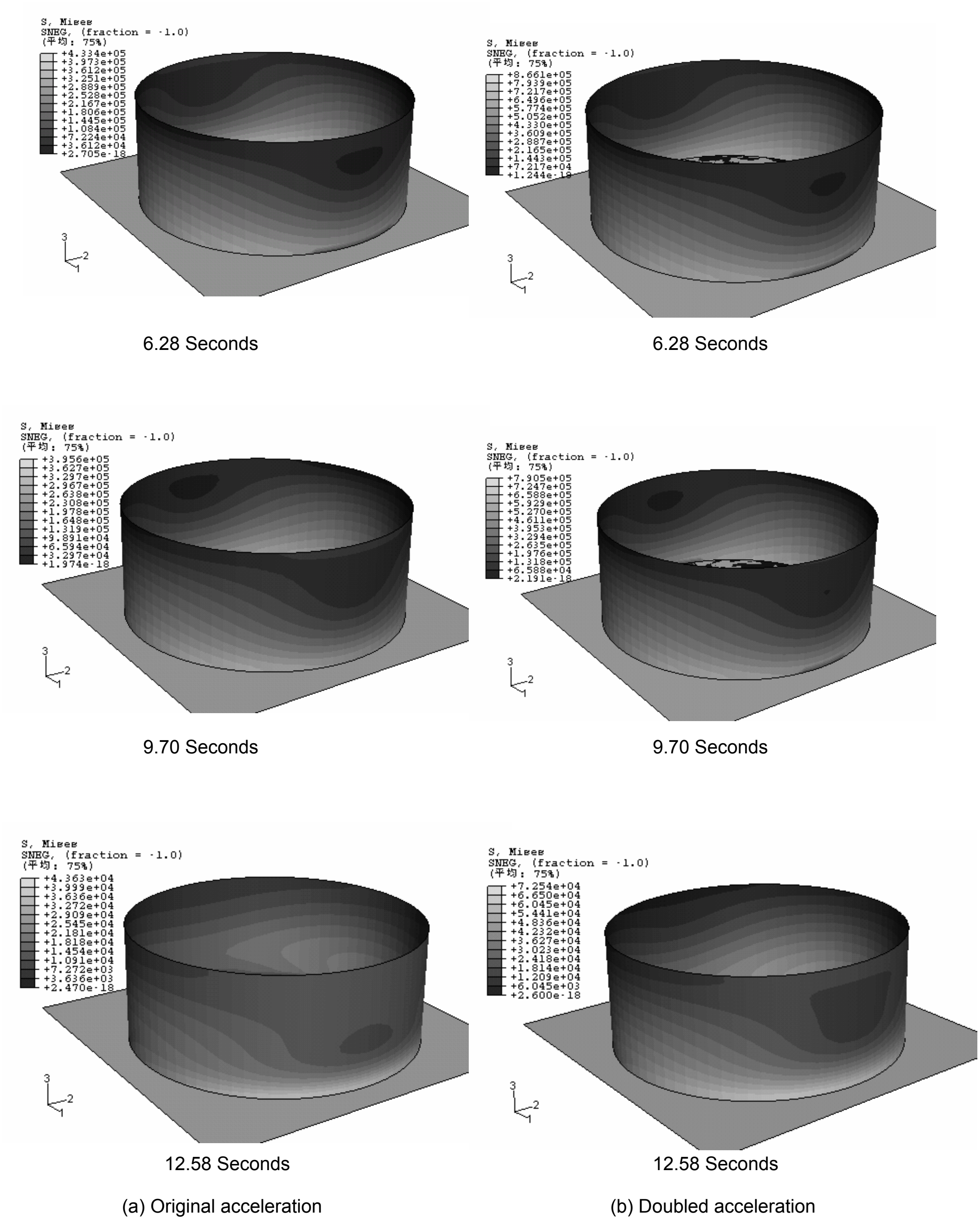

Figure 7. Mises stress of larger tank.

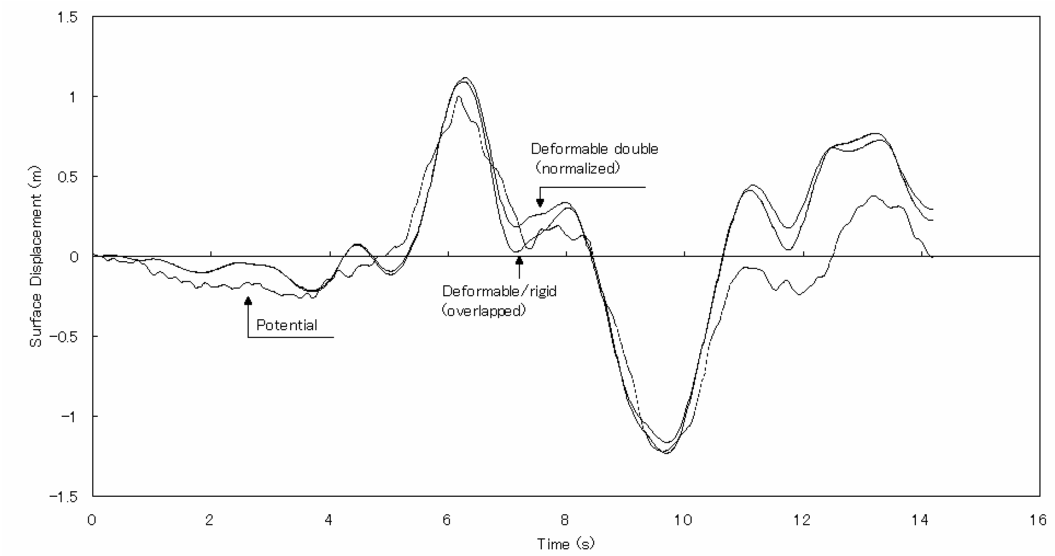

Figure 8. Comparison of liquid surface displacement.

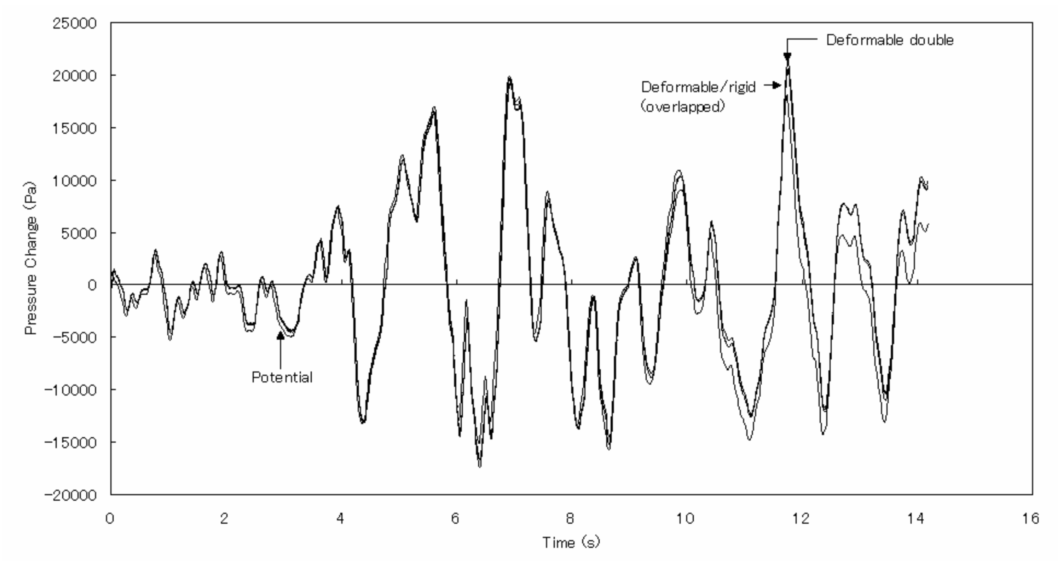

Figure 9. Comparison of liquid bottom pressure.

ΔP : Pressure change [Pa]
η : Surface displacement [m]
r : Horizontal distance from the center of tank [m]
θ : Angle from the motion axis [rad]
z : Vertical position [m]
t : Time [s]
R : Inner radius of tank [m]
H : Liquid level [m]
ρ : Density of fluid [kg/m^3]
g : Gravity acceleration = 9.81 [m/s^2]
ω_i : ith angular eigenfrequency of liquid [Hz]
J_1 : 1st - order bessel function of the first kind
ε_i : Positive root of $\dfrac{dJ_1(x)}{dx} = 0 \ (0 < \varepsilon_1 < \varepsilon_2 \cdots\cdots < \varepsilon_{\mathrm{i}} < \varepsilon_{\mathrm{i+1}})$
$\ddot{x}$: Earthquake acceleration [m/s^2]
ζ : Damping ratio [-]

In these analyses, the wall stiffness is quite high and the result of rigid tank and the deformable tanks agrees quite well when FSI analyses are performed. However it clearly shows that the potential theory does not agree so much with the FSI analyses. It tells that, when sloshing is considered for earthquake, the wall can be assumed rigid and the wave can be obtained. However, FSI type of analyses is required to know the exact behavior of the tank.

6. Conclusion

As the result, the following conclusions were obtained:
(1) Sloshing analyses based on the recorded real earthquake could be done using the FSI capability supported by Abaqus and Fluent via MpCCI.

(2) The FSI analysis results of rigid structure and deformable structure are slightly different, and they do not always agree to the potential theory analyses. It verifies the effectiveness of FSI.

References

1. ABAQUS, ABAQUS Analysis User's Manual, 2006

2. FLUENT, "Fluent 6.2 User's Guide", 2005

3. Housner, G. W., "Earthquake Pressure on Fluid Containers", Eighth technical report under Office of Naval Research, 1954

4. Jacobsen, L. S., "Impulsive hydrodynamics of fluid inside a cylindrical tank and fluid surrounding a cylindrical pier", Bulletin of the Seismological Society of America, 1949

5. KHK (High Pressure Gas Safety Institute of Japan), "Guideline for the Seismic Design of the high Pressure Gas Facilities" KHK E 012-1-2006, 2006 (in Japanese)

6. SCAI (Fraunhofer Institute for Algorithms and Scientific Computing), "MpCCI 3.0 User Manual", 2006

7. YNU (Yokohama National University), "Technical report for strategic operational management of onshore tanks (phase 1)", 2007